JOURNAL OF THE ROYAL SOCIETY Interface

Mineral minimization in nature's alternative teeth

Christopher C Broomell, Rashda K Khan, Dana N Moses, Ali Miserez, Michael G Pontin, Galen D Stucky, Frank W Zok and J. Herbert Waite

J. R. Soc. Interface 2007 **4**, 19-31
doi: 10.1098/rsif.2006.0153

JOURNAL OF THE ROYAL SOCIETY Interface

J. R. Soc. Interface (2007) **4**, 19–31
doi:10.1098/rsif.2006.0153
Published online 5 September 2006

REVIEW

Mineral minimization in nature's alternative teeth

Christopher C. Broomell[1,†], Rashda K. Khan[2,†], Dana N. Moses[3,†], Ali Miserez[4,†], Michael G. Pontin[4,†], Galen D. Stucky[2,3,4], Frank W. Zok[4] and J. Herbert Waite[1,2,3,*]

[1]*Department of Molecular Cell & Developmental Biology,* [2]*Department of Chemistry & Biochemistry,* [3]*Biomolecular Science & Engineering Program, and* [4]*Materials Department, University of California, Santa Barbara, CA 93106, USA*

Contrary to conventional wisdom, mineralization is not the only strategy evolved for the formation of hard, stiff materials. Indeed, the sclerotized mouthparts of marine invertebrates exhibit Young's modulus and hardness approaching 10 and 1 GPa, respectively, with little to no help from mineralization. Based on biochemical analyses, three of these mouthparts, the jaws of glycerid and nereid polychaetes and a squid beak, reveal a largely organic composition dominated by glycine- and histidine-rich proteins. Despite the well-known metal ion binding by the imidazole side-chain of histidine and the suggestion that this interaction provides mechanical support in nereid jaws, there is at present no universal molecular explanation for the relationship of histidine to mechanical properties in these sclerotized structures.

Keywords: histidine-rich proteins; sclerotins; polychaete jaws; squid beak; zinc; copper

1. INTRODUCTION

Impact and wear resistant structures evolved by living organisms encompass some of the most ingenious and fearsome adaptations in hard tissue biology. Scorpion stingers, hydroid nematocysts, snapping claws, fangs, beaks, hooves, ovipositors and antlers represent just a few (Brown 1975). Ostensibly, these structures can be divided into two groups—those with mineral and those without. This is, of course, a naive classification because the boundary between the two is not an abrupt one. Rather, the proportion of mineral and organic phases is an evolutionarily adjustable continuum, and nature undoubtedly possesses examples for every step between all mineral and all organic. Highly mineralized (greater than 50%) impact structures, particularly teeth, have been extensively studied in structural, chemical, mechanical and clinical detail. However, much less is known about the more diverse non- or slightly mineralized structures. Indeed, given the widely held view that mechanical robustness is imparted by the presence of hard minerals, non-mineralized structures have typically been dismissed—at least as bio-inspired design paradigms for hard, abrasion resistant materials. One chink in the 'armor' occurred when Lichtenegger *et al.* (2002) reported that the abrasion resistance of *Glycera* jaws was tantamount to that of tooth enamel, yet with only a tenth as much mineral. This was followed by another report that hardness and stiffness in the completely non-mineralized jaw of *Nereis* approach those of tooth dentin (Lichtenegger *et al.* 2003). Thus, a new research hypothesis is emerging: that factors other than mineral content can endow biological materials with stiffness, hardness and abrasion resistance. The practical significance of this cannot be emphasized enough.

In this review, we describe some of the recent advances in the biochemical, structural and mechanical characterization of three impact structures: jaws from two marine polychaetes (*Glycera dibranchiata* and *Nereis* species) and the beak of the jumbo squid (*Dosidicus gigas*). Of these, only the *Glycera* jaws contain a small amount of mineral, *Nereis* jaws contain Zn ions but no mineral, and *Dosidicus* beak has no detectable inorganic content. These systems are of interest not only for their functional prowess, but also because they serve as possible models for a new generation of bio-inspired, mechanically robust materials. Extensive improvements in the repertory of nanocharacterization are providing an ever clearer view of the remarkable chemistry and construction of these materials. This overview is devoted to a brief description of two intimately intertwined topics: the unusual properties of these largely organic sclerotized structures and the evolving technologies available for their characterization.

*Author for correspondence (waite@lifesci.ucsb.edu).
†These authors contributed equally to the study.

Received 4 July 2006
Accepted 1 August 2006

2. CURRENT STRATEGIES FOR MATERIALS CHARACTERIZATION

2.1. Mechanical

Obtaining accurate mechanical property data for biological materials is complicated by several factors. (i) Sample volumes are typically very small. Polychaete jaws, for example, are only about 1–5 mm in size. (ii) Variations in mechanical properties over small length-scales (10–100 μm) are not uncommon. In such cases, macroscopic measurements are, at best, representative of average properties and can only be correlated with average compositions and structural characteristics. (iii) Even when available in large sizes, most biological samples come in complex shapes. Consequently, testing of samples with well-defined geometries, as done for engineering materials, is rarely possible.

Some of these difficulties have been mitigated by recent advances in low-load instrumented nanoindenters. Nanoindentation enables probing of mechanical properties at small length-scales (approx. 1 μm) and is the preferred method for characterizing hard tissues (Pharr 1998; Fisher-Cripps 2002; Oliver & Pharr 2004). The instruments employ high-resolution actuators and transducers to continuously control and monitor loads and displacements on a rigid tip as it penetrates into the surface of a material. Typical measurement resolutions are 100 nN for force and 1 nm for displacement (Fisher-Cripps 2002).

Given the low displacements and forces obtained during nanoindentation, the surfaces of the test specimens must be extremely flat and smooth to ensure accurate measurements. A useful strategy for preparing surfaces with minimal roughness is ultramicrotomy. Just as in the preparation of thin sections for transmission electron microscopy (TEM), the test sample is embedded in a hard resin and the surface is cut or shaved with successively finer glass or diamond knives. The freshly exposed finished surface is then tested. Alternatively, in larger samples (greater than or equal to a few millimetre square), surfaces can be prepared by lapidary polishing. In this case, the sample is embedded in an epoxy resin and subsequently polished with abrasive media of progressively finer grit, typically down to about 0.02 μm.

Nanoindentation is most commonly used to measure the hardness, H, and the Young modulus, E. Both are readily obtained from a single indentation test (Oliver & Pharr 1992). Furthermore, by performing a series of indentation tests at prescribed locations on the specimen surface, mechanical property maps can be generated and correlated to local structure and composition. Additionally, to assess the effects of hydration on mechanical properties, fluid cells can be used to test samples that are fully submerged in a liquid environment (Broomell *et al.* 2006).

Abrasion resistance can also be probed directly using the most recent generations of nanoindenters. For this purpose, two-dimensional transducers are employed to scratch the surface, typically with a sphero-conical indenter tip, while simultaneously measuring the penetration depth as well as both normal and tangential forces (Pontin *et al.* submitted). The results are frequently cast in terms of a (nominal) friction coefficient, defined as the ratio of normal to tangential force. Similarly, wear resistance can be assessed by passing the same indenter repetitively over a prescribed region of the surface. The resulting wear depth is measured *in situ* using a piezoelectric scanner affixed to the transducer.

Like hardness and elastic modulus, fracture toughness K_{Ic} is a critical property in the assessment of structural biomaterials. It is used to characterize a material's resistance to crack propagation, owing to either a global applied force (such as that induced in a jaw during capture of prey) or localized forces that exist at asperity contacts. Indeed, optimizing wear and abrasion resistance requires a balanced combination of H, E and K_{Ic} (Hornbogen 1975; Adachi *et al.* 1997; Budinski 1997). Indentation methods have been used extensively to measure toughness in hard, brittle materials such as ceramics and glasses, but the measurements are predicated on the formation of well-defined cracks, emanating from the edges of the indenter. The critical load to initiate such cracks from the tip of a sharp indenter is proportional to the quantity K_{Ic}^4/H^3 (Lawn 1993). Owing to the combination of low toughness and high hardness characteristic of ceramics and glasses, the crack initiation loads are only moderately high: typically in the range of 0.1–1 N for a Vickers indenter. In contrast, in biological materials, the low hardness leads to exceedingly large critical loads: typically 10^4–10^6 times that for ceramics. Not only are these loads virtually impossible to achieve with current instruments, but also they would lead to indent sizes that dwarf the sample dimensions if applied. Consequently, indentation methods are not a viable option for measuring toughness of most biological materials. Instead, standard (macroscopic) engineering tests on notched test specimens must be performed. The paucity of insect cuticles and other sclerotized structures with adequate dimensions for toughness measurements has led to a rather thin database in comparison to other biological materials (Vincent 2002; Vincent & Wegst 2004).

2.2. Structural characterization

Neither scanning electron microscopy (SEM) nor TEM is new to the investigation of biological materials, but both have become indispensable, especially in combination with other types of analysis (figure 1). It is not uncommon, for example, to examine the same sectioned surface by SEM before and after nanoindentation, finally finishing with a chemical analysis such as backscattered electrons (BSE) or energy dispersive X-ray spectroscopy (EDS) for detection of heavy element and specific element distributions, respectively. Successive imaging and re-imaging of sample surfaces enables the compilation of topographical, mechanical and chemical datasets for the same material before and after specific treatments. This has proven especially revealing in the case of *Nereis* jaw sections before and after removal of Zn by chelation and is generally applicable to a wide variety of sample surfaces.

SEM is used most commonly to explore the topography of a sample surface. Information on the organization of various microstructural entities and

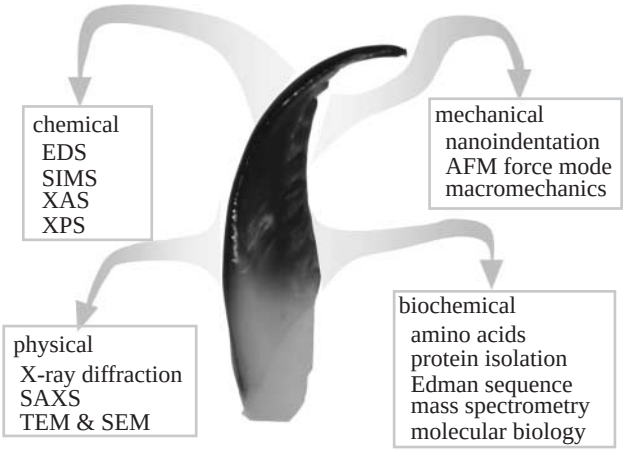

Figure 1. Toolkits for assessing relationships between structure and function in load-bearing abrasion-resistant biological materials.

the micromechanisms of fracture can be obtained by examination of fracture surfaces produced at either ambient or low temperatures. Topography is effectively investigated by secondary electron imaging. In contrast, BSE imaging provides complementary information about the distributions of heavy (electron-dense) elements that frequently reinforce biological materials. Additionally, with the use of EDS and/or electron probe microscopy, maps of elemental distributions in the near-surface regions can be obtained. BSE imaging also lends itself to immunochemistry in that the binding of specific antibodies can be indirectly imaged when coupled to colloidal gold particles (Seto *et al.* 2004).

TEM is well suited for examining the fine structure of thin sections (typically 50–150 nm thick). Samples are fixed and embedded in resin or epoxy in order to preserve the natural structural order. Samples can be non-specifically stained with heavy-metal compounds such as uranyl acetate or osmium tetroxide to provide contrast for general morphological characterization. In addition, they can be labelled with specific antibodies, coupled to electron-dense colloidal gold, for example, to localize individual proteins or other molecules. Although compelling when it works, immunohistochemistry is often less than satisfactory in those materials where sclerotization involves biochemical changes that alter the original antigenic epitopes (Anderson & Waite 2000; Robinson *et al.* 2001). In SEM as in TEM, the biological materials subjected to electron beams emit X-rays, thus enabling determination of additional elemental and chemical information on a nanometer scale (Williams & Carter 1996). Sections of secretory granules (1 µm diameter), for example, have been subjected to EDS for detection of divalent metals (Vovelle & Grasset 1990; Foster *et al.* 1993); selected area electron diffraction of *Glycera* jaw thin sections has revealed higher-order structures such as crystalline fibres of a copper-based mineral (Lichtenegger *et al.* 2002).

Small-angle X-ray scattering (SAXS) has also been used to reveal and quantify fine-scale structural features and their spatial arrangements in hard biological tissues (Fratzl *et al.* 1997; Lichtenegger *et al.* 2003; Gupta *et al.* 2005). With the small diffraction angles (less than 1°) resolvable by SAXS, features at length-scales of 1–100 nm can be readily probed. In both *Glycera* and *Nereis* jaws, for example, SAXS measurements have been used to demonstrate that the atacamite and protein fibres, respectively, are parallel with the long axis of the jaw (Lichtenegger *et al.* 2003, 2005).

2.3. Compositional

2.3.1. Elemental analysis. Despite the variety of available techniques, the hierarchical and multi-dimensional organization of biomolecular materials provides endless surprises and challenges for investigators attempting to define the correlations between structure and composition (figure 1). EDS, secondary ion mass spectrometry (SIMS) and X-ray photoelectron spectroscopy (XPS) enable chemical analysis of a surface and each has different advantages and limitations. In EDS, the incident beam of electrons induces X-rays of characteristic energies to be emitted from the material sample (Williams & Carter 1996). We have applied this technique mostly to microtomed surfaces of biological materials. As previously noted, the main advantage to this approach is the convenience of elemental analysis following nanoindentation, so that hardness and stiffness can be correlated to specific element distributions. In addition, elements can be mapped over the entire sample or along line scans (Birkedal *et al.* 2006; Broomell *et al.* 2006).

SIMS and XPS are common methods for elemental analysis of solid samples (Briggs 1998; Ratner *et al.* 2004) and are useful for determining the compositions of surfaces and interfaces between dissimilar phases. In SIMS, an ion beam is rastered over a defined region of the sample surface, resulting in the generation of secondary ions from resident elements in the material (Briggs 1998; Ratner *et al.* 2004). This is a destructive process, leading to the formation of a crater, which deepens over time. Mass analysis of secondary ions liberated from the sample crater provides elemental depth profiles of surface regions up to 10–20 µm deep, enabling an assessment of the interrelationship of chemical composition and material ultrastructure (Khan *et al.* 2006).

XPS has a depth penetration of less than 100 Å and is thus ideal for characterizing the chemistry of the outermost surface. XPS is conceptually the opposite of EDS; interaction of X-rays with the sample surface induces emission of electrons with energies that are characteristic for each element (Moulder *et al.* 1995; Briggs 1998). In many cases, XPS can be used to deduce the bonding environments of elements detected in biological surfaces. For example, halides can be easily distinguished from organohalogens in *Nereis* jaws (Khan *et al.* 2006). As a rule, sample spectra need to be accumulated quickly to avoid artefacts. Otherwise, during lengthy beam exposures, sample decomposition can be substantial. In *Nereis* jaws, for example, following 60 min of beam exposure, C–X bonds (X being I, Br or Cl) begin to decompose into multiple chemical environments (R. K. Khan 2005, unpublished data).

Although current technology can provide much information about line and depth profiles of elemental composition, information about the distribution of larger functionalities is somewhat more limited. Phenolic groups, such as those in bromo- and iodo-tyrosines in *Nereis* jaws, are readily distinguishable by the influence of phenolic environments on the halogens in XPS (Khan *et al.* 2006), but unhalogenated functionalities like the phenol, imidazole and catechol of tyrosine, histidine and 3,4-dihydroxyphenylalanine (DOPA), respectively, are not. At one time, laser Raman microprobe spectroscopy was expected to fill this void in biological samples (Dong *et al.* 2003; Takeuchi 2003), but the high intrinsic fluorescence of many sclerotized materials including polychaete jaws has prevented its widespread use.

Investigators increasingly subject whole or sectioned biological samples to synchrotron X-ray analysis. These instruments have a positional resolution of 5 µm and are frequently equipped with a variety of characterization tools including X-ray fluorescence, absorption (XAS) and diffraction (Lichtenegger *et al.* 2005). When transition metals are present, XAS can provide exceptional insights about metal bonding environments by excitation of K-edge electrons. Two applications of XAS, namely X-ray absorption of near edge structure (XANES) and more particularly extended X-ray absorption fine structure (EXAFS), often allow a confident reconstruction of the ligand environment around the metal nucleus (Holm *et al.* 1996). EXAFS, which measures the oscillating photoelectron energy of BSE, is less sensitive than XANES but informative about the scattering groups (e.g. ligands) and bond lengths. In the case of the XANES and EXAFS spectra for a *Nereis* jaw tip, an extensive bio-inorganic database (Protein Data Bank) was searched to reveal the best fit; this was found to be the Zn insulin hexamer with three imidazoles and one chloride ligand for each Zn^{+2} nucleus (Lichtenegger *et al.* 2003).

2.3.2. Protein analysis. Biochemical characterization of macromolecules from sclerotized materials has always been daunting. It remains so despite a dramatic increase in the sensitivity of various methodologies. Although difficulties are usually attributed to 'cross-linking' of component molecules, this remains more anecdotal than proven. Many silks, for example, resist characterization despite the absence of cross-links. Techniques employed in the characterization of protein from biological materials include bulk amino acid analysis and peptide mapping in combination with N-terminal (Edman) sequencing (Wilson & Walker 2000; figure 1). Composition analysis allows for qualitative and quantitative characterization of standard amino acids from intact structures or fractions purified from extracts. Quantitative data are useful for assessing the mass percentage of protein in the intact structure, whereas qualitative data provide molar ratios of constitutive residues (excluding asparagine and glutamine). Although no sequence information is given by this technique, composition analysis can, in some cases, provide clues into the nature of a protein component. Characteristic molar ratios between specific amino acids often provide evidence of sequence repeats, such as glycine, proline and hydroxyproline in collagen-like domains, and glycine, alanine and serine in silks. In principle, post-translational modifications can also be identified by comparison with known standards, if available, although corroboration by additional techniques (such as tandem mass spectrometry) is necessary.

Direct sequence determination is achieved by N-terminal sequencing (Edman degradation). Traditionally, complete (or near complete) sequences are obtained by splicing together overlapping peptide sequences generated from multiple digests of purified protein. This often requires the isolation of significant quantities of protein, a rare luxury in scleroproteins. The same processing events, which confer ideal functional properties *in vivo* (insolubility, hardness, resistance to environmental insult, etc.), often render the component proteins intractable to chemical or enzymatic extraction in the laboratory. Additionally, variations in primary sequence within a 'purified' fraction can prevent isolation of enough homogenous sample for a thorough sequencing regimen. Even when a sufficient quantity of material can be purified, traditional Edman degradation is not always informative when unstable post-translational modifications such as phosphoserine dihydroxyproline, γ-carboxyglutamate, sulfotyrosine and others occur (Wold & Moldave eds 1984). Thus, in many cases, the biochemist can only glean small stretches of sequence information of a few peptides from a large protein or complex. This is akin to trying to describe the picture on a jigsaw puzzle from a few miscellaneous pieces. In such cases, molecular biology offers the only recourse for solutions.

Recombinant DNA technology has been a great boon for the characterization of proteins from biological materials. Using well-established techniques, such as polymerase chain reaction with degenerate oligonucleotides, sequence obtained from a small peptide—as few as 6–10 residues—is often sufficient to clone the gene encoding the protein from its associated tissue, thereby allowing the deduction of the full-length protein sequence. This greatly facilitates the analysis of materials with poorly extractable components. Additionally, as these techniques select for any genes (in a given collection of cDNA) that encode the particular sequence, one can often identify variants at the genetic level or, even, proteins with similar sequence motifs (and possibly functions) from closely related organisms.

Although such methodology has greatly facilitated identification of proteins in hopelessly insoluble scleroproteins (Koch *et al.* 1998; Anderson & Waite 2000), it does have significant limitations. As primary sequences are deduced from recombinant DNA, all information reflects only unprocessed precursors. Any modifications present in the native molecule (e.g. hydroxylation, deamidation, cross-linking, halogenation, etc.) cannot be identified. Such modifications can be characterized, however, by comparing deduced sequences to those obtained using modern proteomics techniques (i.e. tandem mass spectroscopy; Taylor *et al.* 1994).

Comparison of peptide masses 'expected' from predicted sequences to those 'observed' from purified peptides occasionally enables identification and localization of modifications in the native molecule.

3. CASE STUDIES

3.1. Squid beaks: chitin-containing composites

Cephalopods are equipped with robust beaks with which they grasp and tear apart food. Comprehensive nomenclature and description of cephalopod beaks can be found in Clarke (1986), whereas a detailed study of the mandibular action has been described in Kear (1994). Given their large size (1–3 cm), *Dosidicus gigas* beaks (figure 2*a*,*b*) lend themselves to a battery of mechanical tests not possible with smaller structures. The dominant microstructural characteristic revealed by optical and scanning electron microscopy is the lamellar organization of the constituents; the lamellae are oriented predominantly towards the tip of the beak and perpendicular to the external beak surface. figure 2*c* is a low magnification image by light microscopy of a fracture surface illustrating this layered structure. The sample was dissected from the external part of the upper beak and the plane of the fracture surface is orthogonal to the beak axis (the tip of the beak being situated above the plane of the sheet). The figure also indicates that the lamellae do not traverse completely through the beak thickness. Evidently, there is a thin coating on the external surface of the beak perpendicular to the lamellae. SEM imaging of fracture surfaces reveals that the lamellae are about 1–3 μm thick (figure 2*d*) and the near-surface layer is about 50 μm thick (figure 2*c*).

Structural features at the nanometer scale have been identified by SAXS. The measurements reveal the presence of fibres (likely chitin) with characteristic dimensions ranging from 5 to 35 nm. They also indicate that the fibres are preferentially oriented along the beak axis in the near-tip regions.

Proteins comprise 40–45% of the dry weight of the beak, as determined by quantitative amino acid analysis. X-ray and EDS studies have confirmed that the beak is devoid of metal ions, minerals and halogens. Chitin has been detected by analysis for amines and wide-angle X-ray scattering and is estimated to be 15–20 wt% (dry) at the beak tip (figure 2). The composition of the remaining 35–40% is unknown. It may be a melanin-like residue, similar to that found in *Glycera* jaws (described later), since a fine insoluble blackish powder always remains after acid hydrolysis. Another intriguing possibility is that the beak contains a high density of aromatic cross-links between peptides and/or chitin, which are not detectable by any of the analytical methods used. Chitin appears to provide a residual scaffold for the beak: when whole beaks are degraded in a H_2O_2/NaOH solution, the hard tissue becomes very soft, featuring a hydrogel-like texture (figure 3), but its overall shape is preserved. Subsequent analysis shows that the degraded structure contains only chitin, whereas pigments and proteins are removed.

A prominent feature of matrix proteins in *Dosidicus* beak is the relative abundance of Gly and His at 25 and 10 mol%, respectively. This composition is strikingly resonant with sclerotized insect cuticles (Andersen *et al.* 1995; Iconomidou *et al.* 2005) as well as the polychaete jaws described later. In insect cuticles, it has been postulated that the covalent bonds between chitin and scleroproteins are mediated through His residues (Schaefer *et al.* 1987; Kerwin *et al.* 1999*b*) and that the enrichment of His in the C-terminal region of cuticular proteins plays an active role in sclerotization (Andersen *et al.* 1995).

Whether they act by dehydration or cross-linking or both, low molecular weight catechols are another prerequisite of sclerotization in insect cuticles. Catechols are present in *Dosidicus* beaks in the form of peptidyl-bound DOPA, a post-translational modification of tyrosine. Preliminary analysis of the beak indicates at least two extractable proteins that contain significant levels of both His and DOPA. DOPA-containing proteins are reminiscent of sclerotization in other molluscan structures, notably byssus (Waite 1990). Oxidation of DOPA to quinone in the beak could contribute to beak pigmentation and intermolecular cross-linking, but this remains to be demonstrated.

Typical profiles of Young's modulus and hardness along a longitudinal section of a beak are shown in figure 4. Although some variation occurs from beak to beak, fairly uniform values are measured on a single specimen. Property gradients like those found in polychaete jaws (Waite *et al.* 2004) have not been detected in the hard regions of the beaks. Typical properties of dry beaks are $E=7$–9 GPa and $H=0.6$–0.8 GPa. These values are similar to those of *Nereis* jaws at Zn contents of 1–2% and are at least twice those of the stiffest and hardest engineering polymers with comparable densities. However, they are significantly lower than those of *Glycera* jaws at the highest mineral content (figure 5). Hydration lowers these property values by about 1/3 to $E\approx 5$ GPa and $H\approx 0.4$ GPa. The fracture toughness K_{Ic} measured on macroscopic fracture specimens are 3.2 ± 1.5 and 3.5 ± 1.1 MPa $\mathrm{m}^{1/2}$ in dry and wet conditions, respectively. Interestingly, despite having a hardness well above that of the hardest engineering polymers, the jaws exhibit a fracture toughness which is comparable to that of the toughest polymers (Kausch *et al.* 2001). This is an unusual combination, in light of the usual trade-offs between toughness and hardness in most engineering materials. Additionally, although the database remains thin, the only known biological structural material that exhibits higher toughness is antler (Zioupos *et al.* 1996; figure 5).

Using the preceding property values, an initial assessment can be made of the abrasion resistance of the beaks. For soft materials (encompassing most engineering polymers and metals as well as the squid beaks), abrasive damage occurs only when the local stress beneath a contact exceeds the material yield strength. The pertinent material property group that characterizes resistance to plastic deformation during contact with a blunt abrasive body can be ascertained from Hertzian contact mechanics (Johnson 1985). The

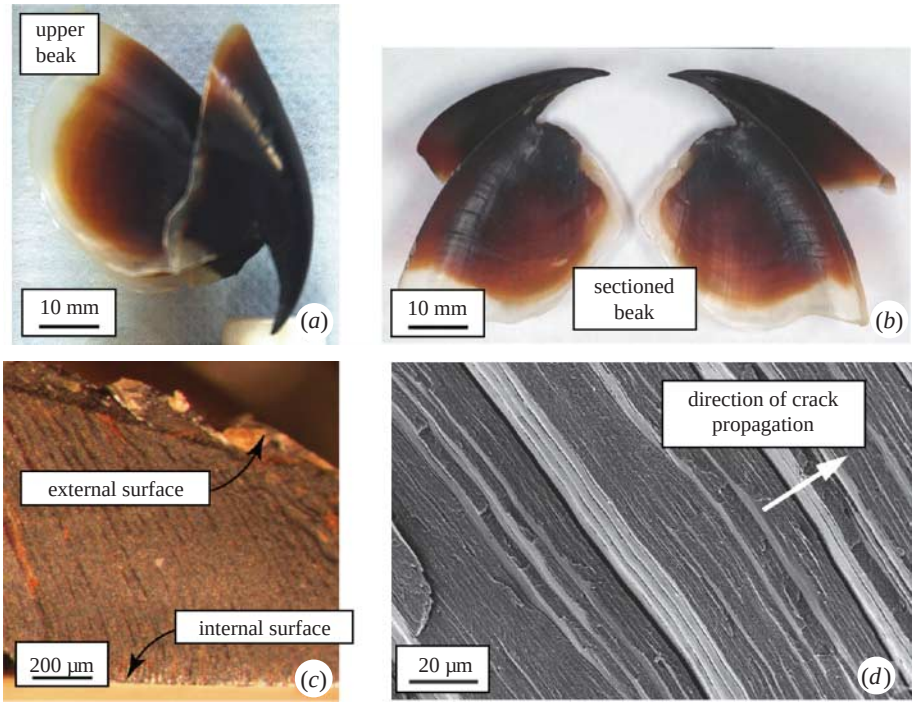

Figure 2. *Dosidicus gigas* beak at various length-scales. (*a*) Beak after dissection from the buccal mass. (*b*) Upper beak after a longitudinal cut along the axis of the beak. (*c*) Fracture surface viewed with a stereo-microscope. (*d*) Higher magnification SEM view of the fracture surface, revealing the layered organization of the structure.

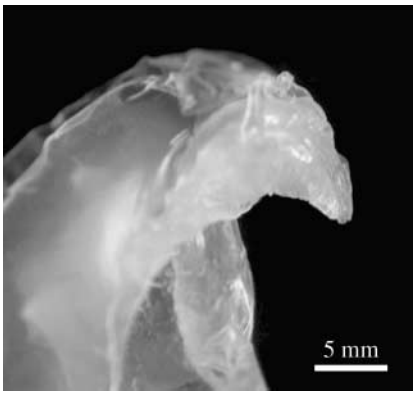

Figure 3. Translucent residue of chitin following extended immersion of *Dosidicus* beak in alkaline peroxide.

resulting critical load for yield initiation is proportional to the material property group H^3/E^2. Comparative assessments of abrasion resistance are made by plotting H versus E for materials of interest. When plotted logarithmically, data lying on a straight line of slope 2/3 represent materials with equivalent performance, i.e. with the same value of the property group and hence the same load for yield initiation. Figure 6 shows such a plot with data for common engineering polymers as well as that for the squid beak. Also shown in the figure is a family of lines of constant H^3/E^2: each one corresponding to dentin (lowest line), polyamide (the best of the engineering polymers) and enamel (top line). The plot reveals that the value of H^3/E^2 for the squid beak is higher than that for dentin and comparable to those of the best engineering polymers. A more critical assessment awaits the outcome of direct abrasion measurements.

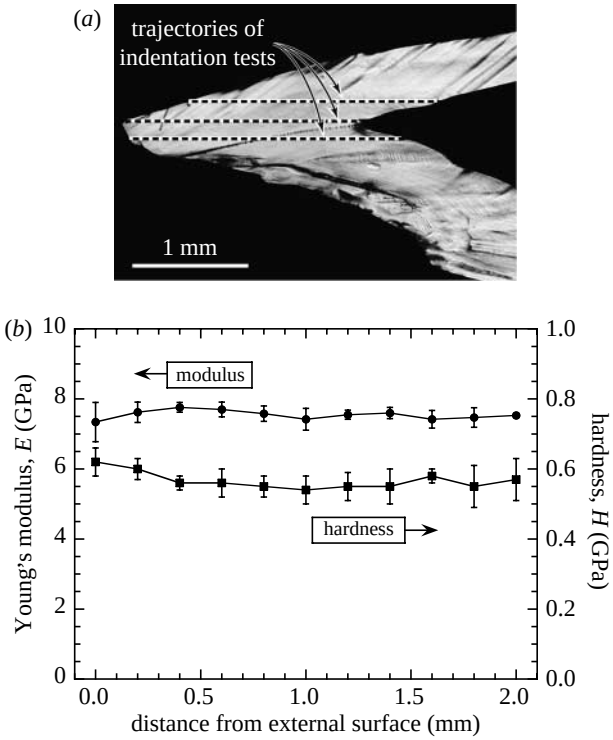

Figure 4. Hardness and modulus profiles measured on a longitudinal section of a *Dosidicus* beak. (*a*) Polished longitudinal section. Horizontal lines represent locations of indent arrays. (*b*) Corresponding modulus and hardness profiles, averaged over the three profiles. Error bars denote standard deviation.

3.2. Nereis jaws: composite of protein and metal ions

Nereid polychaetes are armed with a pair of reversible fang-like jaws that are used for grasping food and

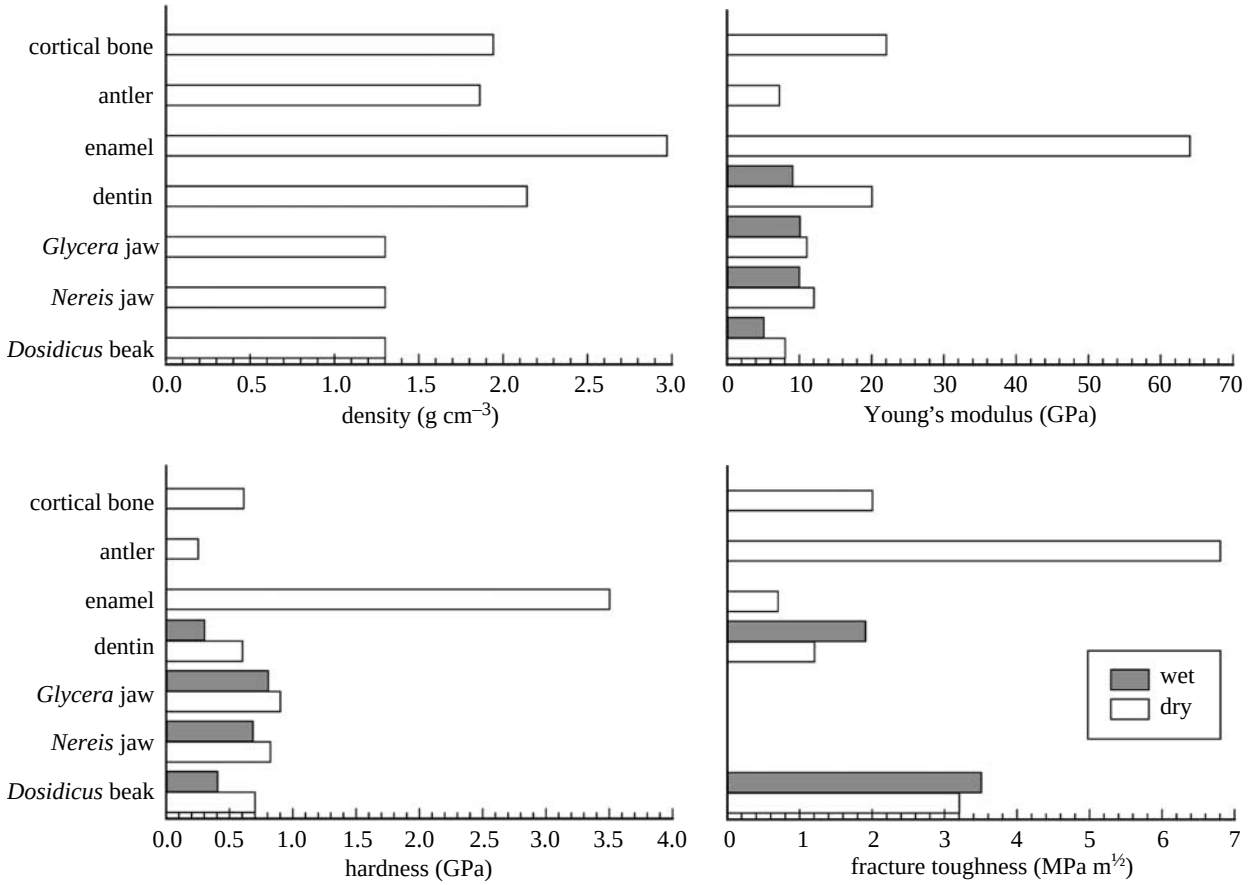

Figure 5. Comparison of physical and mechanical properties of select biomaterials. (Sources of data: *Dosidicus* beak—Miserez *et al.* (2006); *Nereis* jaw—Broomell *et al.* (2006); *Glycera* jaw—Moses *et al.* (2006); dentin—Kinney *et al.* (2003) and Kruzic *et al.* (2003); enamel—Marshall *et al.* (2001); antler—Zioupos *et al.* (1996) and Currey (1999); cortical bone—Rho *et al.* (1997) and Nalla *et al.* (2004)).

defence (figure 7*a*,*b*). The jaws of *Nereis virens* are complex with respect to architecture and composition. Structurally, they approximate fibre-reinforced composites with bundles of fibres arranged parallel to the contour of the jaw's long axis (figure 7*c*). SAXS analysis indicates that the fibres are themselves arrays of tightly packed fibrils, each with a diameter of roughly 50–100 nm (Lichtenegger *et al.* 2003). The jaw is encased within an amorphous coating (3–10 μm thick) of unknown composition (figure 7*b*).

Nereis jaws contain protein, metal ions and the halogens Br, Cl and I; each differentially distributed throughout the structure (Lichtenegger *et al.* 2003; Birkedal *et al.* 2006; Khan *et al.* 2006). The distributions of Br, I and Cl were explored near the jaw tip using SIMS from the surface to a depth of about 10 μm and found to be deficient in the first 1–2 μm (figure 7*d*). Protein is the most abundant constituent, comprising between 70 and 90% of the total mass. Since estimating the proportion of protein is done by amino acid analysis, all post-translational modifications resulting in derivatives not recognized or detected by the analyser would lower the estimated percentage by weight. Amino acid content is biased towards glycine and histidine (36 and 19 mol%, respectively, in whole jaws; Broomell *et al.* 2006), whereas, as revealed by analysis of small jaw sections, important differences in the content of some residues exist. Figure 8

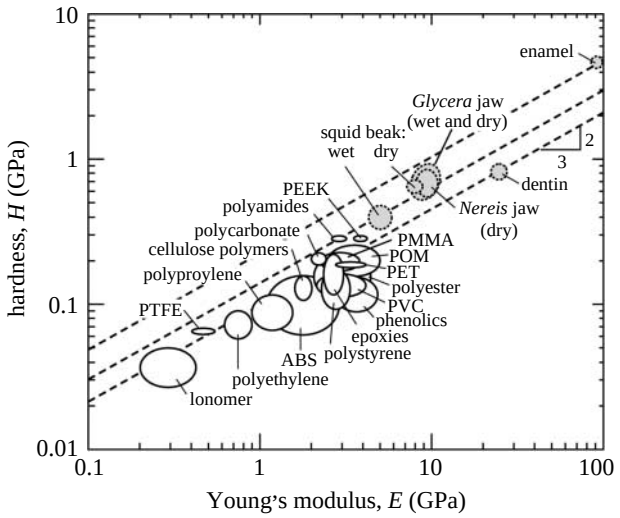

Figure 6. Property maps showing resistance to yielding at blunt contacts with no friction, for rigid abrasives.

demonstrates that histidine concentration increases towards the tip and toothed-edge of the jaw (Birkedal *et al.* 2006). The opposite trend is observed for alanine; levels increase towards the jaw base. Concentrations of other predominant amino acids (tyrosine and aspartate) do not vary within the jaw. These results suggest that the jaw is made up of at least two, but probably more, proteins with distinct compositions and distribution

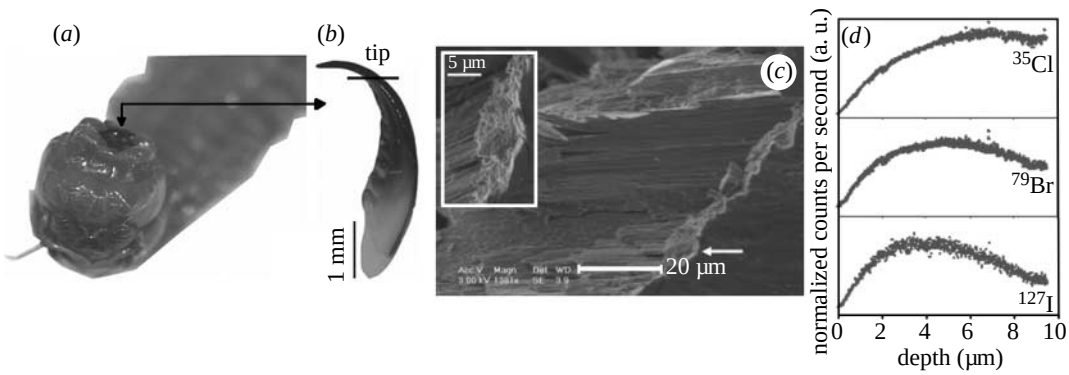

Figure 7. Structure and composition of *Nereis* jaws. (*a*) Typical position of jaws in a distended proboscis. (*b*) Optical micrograph of a dissected *Nereis* jaw (scale bar, 1 mm). (*c*) Scanning electron micrograph of a fracture surface near the jaw tip showing the outer cuticle (arrow) and underlying fibrous composite. (*d*) SIMS analyses made at the line indicated in (*b*). All three halogens are depleted in the near-surface region. The chlorine plateau is sustained whereas Br and I return towards baseline after peaking.

profiles. Extractable protein accounts for only 0.1% of the total jaw mass. The major protein extractable from the jaw has a mass of about 35 kDa and a composition in which both glycine and histidine approach 30 mol% (Broomell & Waite in preparation). This is likely to predominate at the tip.

Recent evidence suggests considerable post-translational modification of nereid jaw proteins. Halogenation of both tyrosine and histidine are prevalent, but DOPA and aryl coupling products, e.g. di- and trityrosines, are also detectable (Birkedal *et al.* 2006). The biochemical reactions responsible for these modifications in the jaws have not yet been determined. Both halogenation and cross-linking of tyrosine residues are often mediated by peroxidase activity, which has been histochemically detected *in situ* (Edelhoch & Lippoldt 1962; C. Broomell, unpublished data). It is possible that either modification is a byproduct of the other (i.e. intentional cross-linking results in inadvertent halogenation or vice versa). However, the distinct distribution of each halogen suggests that jaw protein modification involves multiple specific processes. Although the functional consequences of such activity are unclear, a multi-step modification process may be advantageous for two main reasons: (i) mechanical/chemical properties can be changed at the regional level without having to change the general protein expression profile and (ii) properties can be modulated later in development (i.e. after jaw material is deposited), perhaps assisting with remodelling or repair. Establishment of halogenation at the jaw periphery, for example, could diminish susceptibility to degradation by chemical or microbial attack (Myneni 2002).

Non-mineral Zn accounts for roughly 2% of the total jaw mass (Bryan & Gibbs 1979*a*). Results of X-ray absorption spectroscopy suggest a single metal coordination environment with each Zn ion bound by three histidine residues and a chloride ion thereby resembling the coordination environment in the Zn insulin hexamer (Lichtenegger *et al.* 2003). Since early studies on the composition of *Nereis* jaws were conducted on specimens from polluted estuaries in the UK, it was initially proposed that the jaws might serve as a metal-sink, sequestering toxic levels of Zn absorbed from the sediment away from the living tissue (Bryan & Gibbs 1979*b*). Further observations demonstrated that Zn levels in jaws were high, regardless of environmental context, leading to the hypothesis that metals might contribute to their mechanical properties. Several lines of evidence support this hypothesis. Zn levels increase (approaching 10%) towards the tip and toothed-edges of the jaw—both regions that need to be hard *in vivo*. Both hardness and modulus increase with Zn content in jaws (Lichtenegger *et al.* 2003). Most importantly, removal of Zn by chelation with EDTA causes a nearly 80% reduction in both H and E (Broomell *et al.* 2006). Both properties are almost completely restored following reintroduction of Zn into the jaw matrix (figure 9). Taken together, these data support the view that Zn is an essential ingredient for endowing the *Nereis* jaw with its mechanical robustness.

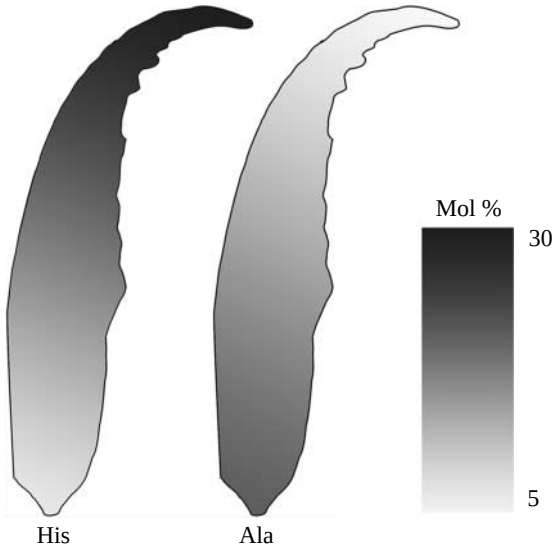

Figure 8. Distributions of histidine and alanine within the jaw of *Nereis*. Since the only known jaw precursor, nvjp-1, is rich in histidine but not alanine, the gradients are suggestive of another protein gradient. Adapted from Birkedal *et al.* (2006).

A comparison of H and E for *Nereis* jaw tips with other biomaterials and polymers is shown in figures 5 and 6. As for the squid beak, the expected abrasion resistance, characterized by H^3/E^2, is higher than that for dentin and comparable to that of the best engineering polymers.

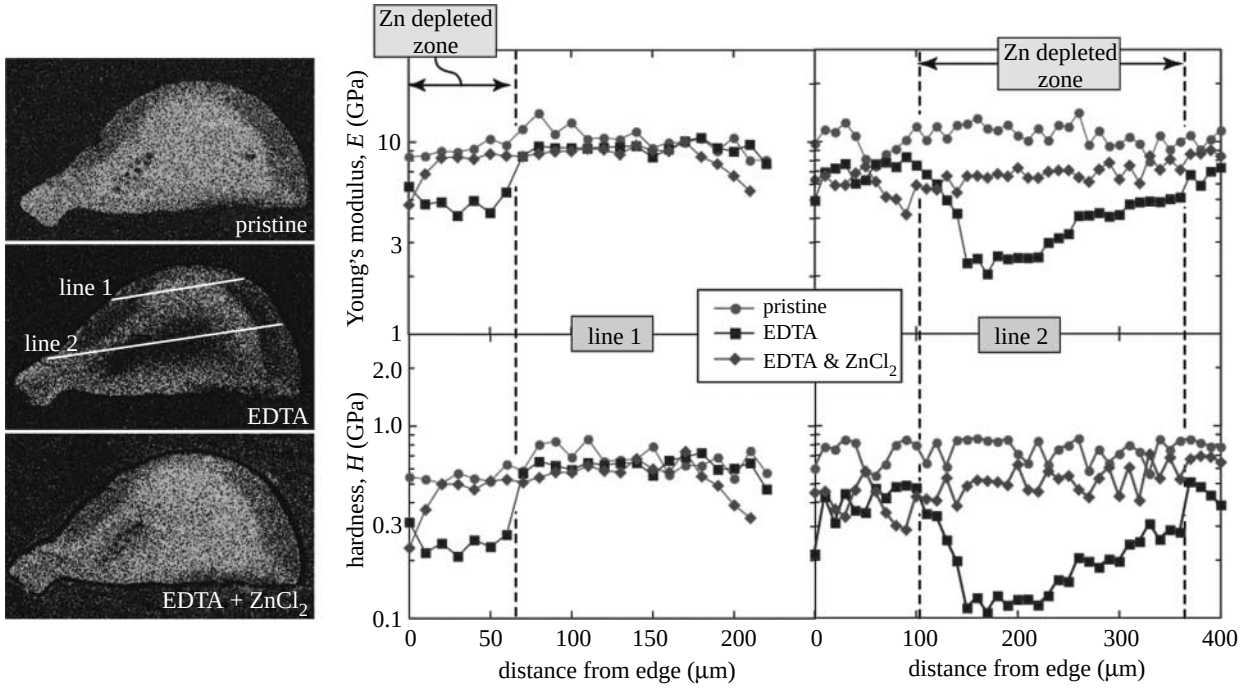

Figure 9. (*a*) Zn distribution in a sectioned jaw of *Nereis*, showing effects of EDTA treatment and Zn re-constitution following chelation. The two lines denote nanoindentation trajectories. (*b*) Corresponding modulus and hardness profiles showing large property reductions in regions of significant Zn depletion. Adapted from Broomell *et al.* (2006).

3.3. Glycera jaws: composite of protein, melanin, mineral and metal ions

The four fangs comprising the jaw of the marine worm *Glycera* are instruments that serve the dual purpose of grasping and injection. The fangs are hollow, like a syringe, with one major and several accessory apertures for release of venom (figure 10*a*; Michel 1970; Meunier *et al.* 2002). The jaws consist of melanin, protein, atacamite mineral ($Cu_2Cl(OH)_3$) and Cu ions (Gibbs & Bryan 1979; Lichtenegger *et al.* 2002, 2005; Moses *et al.* in press). Melanin comprises about 40% of the jaws by dry weight. Moreover, it exists as a contiguous phase throughout the jaw and is arranged in sheets approximately 200 nm thick, oriented perpendicular to the long axis of the jaw (Moses *et al.* submitted; figure 10*a*). Protein comprises 40–45% of the jaws by dry weight. Although the protein is distributed throughout the jaws, the His content is elevated near the jaw tips, where it approaches 25 mol%. A high degree of chemical and physical intimacy between the His-rich domains of the protein and the melanin is suggested by the fact that, following exhaustive hydrolytic removal of all proteins, the remaining microstructure still retains the essential features of the pristine jaw (Moses *et al.* in press). Atacamite mineral accounts for less than 10% of the jaws by dry weight. The mineral is arranged as fine fibres, located near the outer surfaces of the jaw tip and oriented parallel to the outer surface (Lichtenegger *et al.* 2002). Distinct from atacamite, Cu ions also appear to be localized to the near-surface layers in the jaw tips (figure 10*b*; Lichtenegger *et al.* 2005).

Given the relatively sparse mineralization, the high stiffness of *Glycera* jaws suggests a densely cross-linked structure. Assuming that Cu ions play a role analogous to that of Zn in *Nereis* jaws, we have been keen to measure the mechanical consequences of Cu removal. Unfortunately, typical chelate-based metal ion depletion strategies do not dislodge Cu ions from *Glycera* jaws. While EDTA treatments for 3 days typically suffice to demineralize bone and teeth and remove Zn from *Nereis* jaws, EDTA treatment of *Glycera* jaws for as long as 2 weeks does not remove detectable levels of Cu (Moses *et al.* 2006; figure 10*c*). It is unlikely that the affinity of Cu binding to His-rich domains would exceed that of Cu–EDTA (Dawson *et al.* 1986), but the extreme stability of the Cu–melanin complex is well known (Szpoganicz *et al.* 2002). At present, we propose that at least some of the Cu connects the melanin to which it is tightly bound and the His-rich domains to which it is less tightly coordinated. It does not seem probable that Cu cross-links melanin polymers in the jaws because the melanin component was still stiff after the metal (and everything else) had been removed by extended hydrolysis in strong acid. The remarkable cohesion within the melanin of the jaw has been attributed to π–π interactions in the interior and H-bonding along the edges of stacked, highly aromatic sheets of polyhydroxyindoles (Stark *et al.* 2005). Whether the high aromaticity or degree of cross-linking mitigates the mechanical response of jaws to hydration is not known; although the hardness and modulus of human dentin exhibit 50% reductions when hydrated, the corresponding property changes in *Glycera* jaws are only about 20% (Ho *et al.* 2004; Moses *et al.* 2006).

Nanoindentation tests indicate that the highest values of H (0.8–0.9 GPa) and E (9–10 GPa) are obtained in regions with high Cu and Cl content (figure 11). The implication is that atacamite fibres

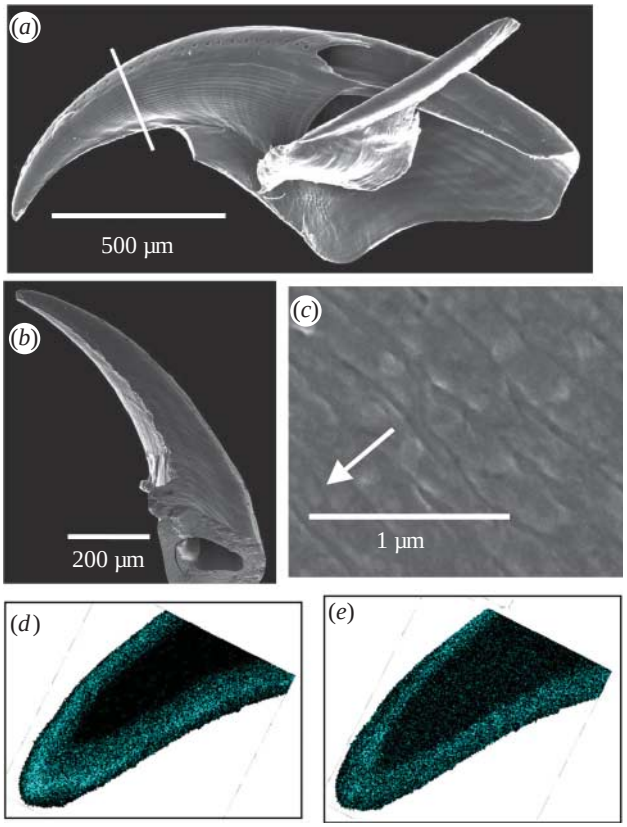

Figure 10. (*a*) Scanning electron micrograph of an untreated *Glycera* jaw. A series of fine venom pores is evident along the upper ridge. (*b*) Scanning electron micrograph of a *Glycera* jaw fractured perpendicular to the long axis of the jaw, at the location of the line in (*a*). The major distal aperture for venom delivery is visible at the bottom. (*c*) Scanning electron micrograph of the fracture surface, showing 200 nm thick sheets of melanin. The sheets are oriented perpendicular to the long axis of the jaw, represented by the arrow. (*d*) Cu map on a longitudinal section through the near-tip region of the jaw. Cu is localized in the near-surface regions. (*e*) Corresponding Cu map following EDTA treatment (same region as in (*d*)). Evidently, EDTA is not an effective Cu chelator in *Glycera* jaws.

and Cu ions near the jaw tip play a significant structural role (Moses *et al.* 2006). This hypothesis is further supported by the observation that these ions are most abundant in the near-surface regions of the jaw tips; precisely where the abrasive forces will be highest during penetration into prey and hence the mechanical properties will be most crucial. Additionally, nanoindentation tests performed on the acid-resistant melanin relics of *Glycera* jaws indicate that both the hardness and the modulus of the melanin alone are approximately one-half of those of the pristine structure (Moses *et al.* 2006). The retention of the jaw shape following exhaustive hydrolysis suggests that the hydrolysed constituents (including minerals, metal ions and proteins) intercalate and interpenetrate a contiguous melanin scaffold (Moses *et al.* submitted). The implications of these arrangements for mechanical robustness have yet to be ascertained.

Based on property measurements under both wet and dry conditions, *Glycera* jaws exhibit similar mechanical characteristics to those of the *Nereis* jaws (figures 5 and 6). Hence, their abrasion resistance is expected to be similar as well.

4. CONCLUSIONS

The hardened mouthparts of two polychaete worms and a squid share similar mechanical properties and protein compositions rich in glycine and histidine. The histidine content—ranging from 12 to 25 mol%—is elevated well above the protein average of 2% (Creighton 1993), thus suggesting a role crucial in function. Histidine serves many pivotal roles in protein function including catalysis (histidine containing triads and metal prostheses), metal storage and detoxification (histidine ligands), and pH-dependent triggers of conformational change (histidine ionization). While it is probable that histidine-rich proteins have been adaptively co-opted by these organisms to optimize some aspect of jaw performance, there does not appear to be a single underlying mechanism for accomplishing this end.

In *Nereis*, a major matrix protein with histidine levels at 30 mol% appears to be a polydentate ligand for Zn^{+2}. Both hardness and stiffness are greatly reduced by the removal of Zn^{+2} and restored by re-exposure to Zn^{+2}. Zn^{+2} is thus a *reversible* cross-linker, in contrast to the dityrosines also present in the structure. Despite the abundance of histidine in *Dosidicus* beak proteins, no metals are present. The sclerotization of beak may parallel histidine-rich insect cuticles, where histidyl side chains are proposed to be nucleophiles of catechol-derived quinones that lead to covalent cross-links (Kerwin *et al.* 1999*a*). While plausible, this hypothesis remains largely unproven. Strong hydrogen bonding between histidine and polyphenols is also possible (Wróblewski *et al.* 2001). Like insect cuticles, squid beak contains both catechols (in the form of peptidyl-DOPA) and chitin (Hunt & Nixon 1981).

The picture is even more complex in the jaws of *Glycera*, where histidine-rich proteins coexist with melanin, mineral and Cu ions (figure 12). The contribution of Cu ions to hardness and stiffness is difficult to ascertain, since no known chelator is strong enough to dislodge the Cu. Moreover, even after exhaustive acid hydrolysis has removed all the protein, mineral and metal ions, the remaining melanin retains over 50% of the hardness and stiffness of pristine jaws.

This review of structure–property relationships has focused on compositional structure, particularly with regard to histidine content. Fibre orientation is also of tremendous importance to fracture toughness in biocomposites (Neville 1993; Currey 2002). Of the three materials covered, only *Dosidicus* beak was large enough to allow toughness measurements and the observed magnitude of these is quite consistent with the laminate construction (figure 2) that is reminiscent of stiff insect cuticles, e.g. locust femur (Neville 1993). Indeed, preferential fibre orientation is evident in all three structures from the tightly bundled fibres of *Nereis* jaws to the neatly stacked lamellae in both *Glycera* and *Dosidicus* jaws (figures 2, 7 and 10). While in *Nereis* jaw the His-rich proteins may contribute to both the fibre and the matrix, in *Glycera* and *Dosidicus* the His-rich proteins appear to be dispersed between the melanin sheets and chitin fibres, respectively, which form the continuous network. A comprehensive study

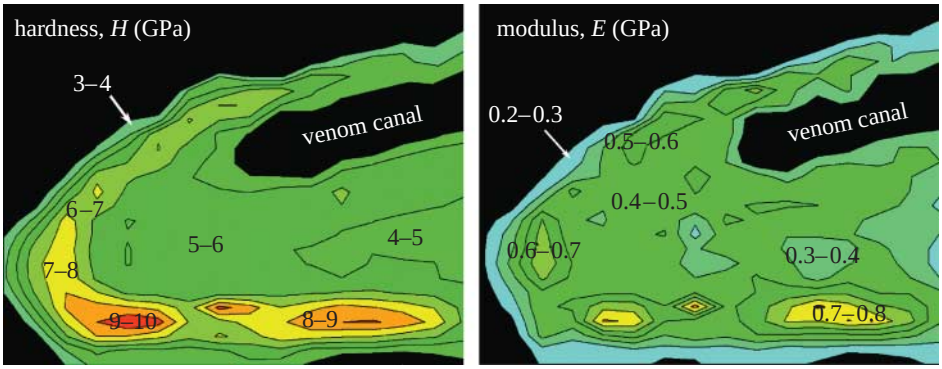

Figure 11. Hardness and modulus maps of the tip region of a *Glycera* jaw, measured while the sample was submerged in water. The regions of high hardness and modulus near the surface are rich in Cu and Cl. Adapted from Moses *et al.* (2006).

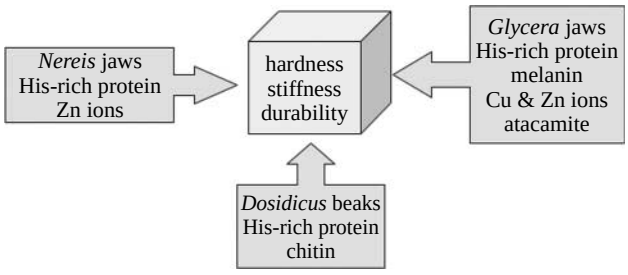

Figure 12. Glycine and histidine (HIS)-rich proteins appear to be unusually versatile for combining with minerals, metal ions and other organic polymers like chitin or melanin for construction of load-bearing sclerotized materials. Fibre orientation would add another level for controlling properties.

of the interrelationships between architecture at different scales and the nanomechanical properties of these materials remains to be done.

In summary, histidine plays as diverse a role in stabilizing the load-bearing biomacromolecules of *Nereis*, *Glycera* and *Dosidicus* as it does in proteins generally. Further exploration of the functional versatility of imidazoles in molecular scaffolds is expected to yield new insights into the mechanisms through which mechanical functionality is endowed in non-mineralized structures. Although it would be a mistake to assume that all load- and impact-bearing structures contain histidine-rich proteins, their occurrence in other load-bearing biomaterials is noteworthy. For instance, a histidine-rich protein, amelogenin, is the major organic component in tooth enamel (Paine *et al.* 2001), and spinalin, with nearly 20 mol% histidine, dominates the ballistic nematocyst spines of *Hydra* (Koch *et al.* 1998).

We thank the National Institutes of Health for a Bioengineering Research Partnership grant (R01 DE014672) and the NASA University Research Engineering & Technology Institute on BioMaterials under award no. NCC-1-02037. A.M. and R.K.K. acknowledge fellowships from the Swiss National Science Foundation (no. PBEL2-104421) and the Graduate Research and Education in Adaptive bio-Technology (GREAT) Training Program of the UC Systemwide Biotechnology Research and Education Program (no. 2005-240), respectively. Characterizations were done with facilities in the Materials Research Laboratory (MRL) at UCSB and supported by the MRSEC Program of the National Science Foundation under award no. DMR00-80034. We thank Dr Cesar Salinas (CIBNOR, La Paz, Mexico) for providing beak samples used in this research.

REFERENCES

Adachi, K., Kato, K. & Chen, N. 1997 Wear map of ceramics. *Wear* **203–204**, 291–301. (doi:10.1016/S0043-1648(96)07363-2)

Anderson, K. E. & Waite, J. H. 2000 Immunolocalization of dpfp-1, a byssal protein of the zebra mussel *Dreissena polymorpha*. *J. Exp. Biol.* **203**, 3065–3073.

Andersen, S. O., Højrup, P. & Roepstorff, P. 1995 Insect cuticular proteins. *Insect Biochem.* **25**, 153–176. (doi:10.1016/0965-1748(94)00052-J)

Birkedal, H., Khan, R. K., Slack, N., Broomell, C., Lichtenegger, H. C., Zok, F., Stucky, G. D. & Waite, J. H. 2006 Halogenated veneers: protein cross-linking and halogenation in the jaws of a marine polychaete worm. *Chem. Biochem.* **7**, 1392–1399. (doi:10.1002/cbic.200600160)

Briggs, D. 1998 *Surface analysis of polymers by XPS and static SIMS*. Cambridge, UK: Cambridge University Press.

Broomell, C. C. & Waite, J. H. In preparation. Isolation and cloning of histidine rich protein from the jaws of *Nereis*, a marine polychaete.

Broomell, C. C., Mattoni, M. A., Zok, F. W. & Waite, J. H. 2006 Critical role of zinc in hardening of *Nereis* jaws. *J. Exp. Biol.* **209**, 3219–3225. (doi:10.1242/jeb.02373)

Brown, C. H. 1975 *Structural materials in animals*. London, UK: Halsted Press.

Bryan, G. W. & Gibbs, P. E. 1979*a* Zinc—a major inorganic component of nereid jaws. *J. Mar. Biol. Ass. UK* **59**, 969–973.

Bryan, G. W. & Gibbs, P. E. 1979*b* Metals in nereid polychaetes: the contribution of metals in the jaws to the total body burden. *J. Mar. Biol. Ass. UK* **60**, 641–654.

Budinski, K. G. 1997 Resistance to particle abrasion of selected plastics. *Wear* **203–204**, 302–309. (doi:10.1016/S0043-1648(96)07346-2)

Clarke, M. R. (ed.) 1986 *A handbook for the identification of Cephalopod beaks*. Oxford, UK: Clarendon Press.

Creighton, T. E. 1993 Proteins, 2nd edn. New York, NY: W. H. Freeman & Company.

Currey, J. D. 1999 The design of mineralised hard tissues for their mechanical functions. *J. Exp. Biol.* **202**, 3285–3294.

Currey, J. D. 2002 *Bones: structure and mechanics*. Princeton, NJ: Princeton University Press.

Dawson, R. M. C., Elliott, D. C., Elliott, W. H. & Jones, K. M. 1986 Data for Biochemical Research, 3rd edn. Oxford: Clarendon Press.

Dong, J., Atwood, C. S., Anderson, V. E., Siedlak, S. L., Smith, M. A., Perry, G. & Carey, P. R. 2003 Metal binding and oxidation of amyloid beta within isolated senile plaque cores: Raman Microscopic evidence. *Biochemistry* **42**, 2768–2773. (doi:10.1021/bi0272151)

Edelhoch, H. & Lippoldt, R. E. 1962 Properties of thyroglobulin: molecular properties of iodinated thyroglobulin. *J. Biol. Chem.* **237**, 2788–2794.

Fisher-Cripps, A. C. 2002 *Nanoindentation*. New York, NY: Springer.

Foster, M. C., Leapman, R. D., Li, M. X. & Atwater, I. 1993 Elemental composition of secretory granules in pancreatic islets of Langerhans. *Biophys. J.* **64**, 525–532.

Fratzl, P., Jakob, H. F., Rinnerthaler, P., Roschger, P. & Klaushofer, K. 1997 Position-resolved small-angle X-ray scattering of complex biological materials. *J. Appl. Crystallogr.* **30**, 765–769. (doi:10.1107/S0021889897001775)

Gibbs, P. E. & Bryan, G. W. 1979 Copper—the major metal component of glycerid polychaete jaws. *J. Mar. Biol. Ass. UK* **60**, 205–214.

Gupta, H. S., Wagermaier, W., Zicker, G. A., Aroush, D. R., Funari, S. S., Roschger, P., Wagner, H. D. & Fratzl, P. 2005 Nanoscale deformation mechanisms in bone. *Nanoletters* **5**, 2108–2111.

Ho, S. P., Balooch, M., Goodis, H. E., Marshall, G. W. & Marshall, S. J. 2004 Ultrastructure and nanomechanical properties of cementum dentin junction. *J. Biomed. Mater. Res.* **68A**, 343–351. (doi:10.1002/jbm.a.20061)

Holm, R. H., Kennepohl, P. & Solomon, E. I. 1996 Structural and functional aspects of metal sites in biology. *Chem. Rev.* **96**, 2239–2314. (doi:10.1021/cr9500390)

Hornbogen, E. 1975 Role of fracture toughness in wear of metals. *Wear* **33**, 251–259. (doi:10.1016/0043-1648(75)90280-X)

Hunt, S. & Nixon, M. 1981 A comparative study of protein composition in the chitin–protein complexes of the beak, pen, sucker disc, radula, and esophageal cuticle of cephalopods. *Comp. Biochem. Physiol. B* **68**, 535–546. (doi:10.1016/0305-0491(81)90071-7)

Iconomidou, V. A., Willis, J. H. & Hamodrakas, S. J. 2005 Unique features of the structural model of "hard" cuticle proteins: Implications for chitin–protein interactions and cross-linking in cuticle. *Insect Biochem.* **35**, 533–560.

Johnson, K. L. 1985 *Contact mechanics*. Cambridge, UK: Cambridge University Press.

Kausch, H. H. Heymans, N., Plummer, C. J. & Decroly, P. 2001 Traité des Matériaux, vol.14. Matériaux Polymères: Propriétés Mécaniques et Physiques, PPUR, Lausanne: Presses Polytechniques et Universitaires Romandes.

Kear, A. J. 1994 Morphology and function of the mandibular muscles in some coleoid cephalopods. *J. Mar. Biol. Ass. UK* **74**, 801–822.

Kerwin, J. L., Turecek, F., Xu, R., Kramer, K. J., Hopkins, T. L., Gatlin, C. L. & Yates, J. R. 1999*a* Mass spectrometric analysis of catechol–histidine adducts from insect cuticle. *Anal. Biochem.* **29**, 229–237. (doi:10.1006/abio.1998.3069)

Kerwin, J. L., Whitney, D. L. & Sheikh, A. 1999*b* Mass spectrometric profiling of glucosamine, glucosamine polymers and their catecholamine adducts. *Insect Biochem. Mol. Biol.* **268**, 599–607. (doi:10.1016/S0965-1748(99)00037-5)

Khan, R. K., Stoimenov, P. K., Mates, T. E., Waite, J. H. & Stucky, G. D. 2006 Exploring gradients of halogens and zinc in the surface and subsurface of *Nereis* Jaws. *Langmuir*, ASAP.

Kinney, J. H., Habelitz, S., Marshall, G. W. & Marshall, S. J. 2003 The importance of intrafibrillar mineralization of collagen on the mechanical properties of dentin. *J. Dent. Res.* **82**, 957–961.

Koch, A. W., Holstein, T. W., Mala, C., Kurz, E., Engel, J. & David, C. N. 1998 Spinalin, a new glycine- and histidine-rich protein in spines of *Hydra* nematocysts. *J. Cell Sci.* **111**, 1545–1554.

Kruzic, J., Nalla, R. K., Kinney, J. H. & Ritchie, R. O. 2003 Crack blunting, crack bridging and resistance-curve fracture mechanics in dentin: effect of hydration. *Biomaterials* **24**, 5209–5221. (doi:10.1016/S0142-9612(03)00458-7)

Lawn, B. R. 1993 *Fracture of brittle solids*, 2nd edn. Cambridge, UK: Cambridge University Press.

Lichtenegger, H. C., Schoberl, T., Bartl, M. H., Waite, J. H. & Stucky, G. D. 2002 High abrasion resistance with sparse mineralization: copper biomineral in worm jaws. *Science* **298**, 389–392. (doi:10.1126/science.1075433)

Lichtenegger, H. C., Schöberl, T., Ruokalainen, J. T., Cross, J. O., Heald, S. M., Birkedal, H., Waite, J. H. & Stucky, G. D. 2003 Zinc and mechanical prowess in the jaws of *Nereis*, a marine worm. *Proc. Natl Acad. Sci. USA* **100**, 9144–9149. (doi:10.1073/pnas.1632658100)

Lichtenegger, H. C., Birkedal, H., Casa, D. M., Cross, J. O., Heald, S. M., Waite, J. H. & Stucky, G. D. 2005 Distribution and role of trace transition metals in *Glycera* worm jaws studied with synchrotron microbeam techniques. *Chem. Mater.* **17**, 2927–2931. (doi:10.1021/cm050233v)

Marshall, G. W., Balooch, M., Gallagher, R. R., Gansky, S. A. & Marshall, S. J. 2001 Mechanical properties of the dentinoenamel junction: AFM studies of nanohardness, elastic modulus, and fracture. *J. Biomed. Mater. Res.* **54**, 87–95. (doi:10.1002/1097-4636(200101)54:1<87::AID-JBM10>3.0.CO;2-Z)

Meunier, F. A., Feng, Z. P., Molgo, J., Zamponi, G. W. & Schiavo, G. 2002 Glycerotoxin from *Glycera convoluta* stimulates neurosecretion by up-regulating N-type Ca^{2+} channel activity. *EMBO J.* **21**, 6733–6743. (doi:10.1093/emboj/cdf677)

Michel, C. 1970 Physiological role of proboscis in four polychætous annelids belonging to genera—*Eulalia*, *Phyllodoce*, *Glycera* and *Notomastus*. *Cah. Biol. Mar.* **9**, 209–228.

Moses, D. N., Harreld, J. H., Stucky, G. D. & Waite, J. H. In press. Melanin and *Glycera* jaws: emerging dark side of a robust biocomposite structure. *J. Biol. Chem.*

Moses, D. N., Mattoni, M. A., Slack, N. L., Waite, J. H. & Zok, F. W. 2006 Role of melanin in mechanical properties of *Glycera* jaws. *Acta Biomaterialia* **2**, 521–530.

Moses, D. N., Harreld, J. H., Mitchell, N. M., Waite, J. H. & Stucky, G. D. Submitted. Nanocomposite ultrastructure of the *Glycera* marine worm jaw.

Moulder, J. F., Stickle, W. F., Sobol, P. E. & Bomben, K. D. 1995 *Handbook of X-ray photoelectron spectroscopy*. Eden Prairie, MN: Physical Electronics.

Myneni, S. C. B. 2002 Formation of stable chlorinated hydrocarbons in weathering plant material. *Science* **295**, 1039–1041. (doi:10.1126/science.1067153)

Nalla, R. K., Kruzic, J., Kinney, J. H. & Ritchie, R. O. 2004 Mechanistic aspects of fracture and R-curve behavior in human cortical bone. *Biomaterials* **26**, 217–231. (doi:10.1016/j.biomaterials.2004.02.017)

Neville, A. C. 1993 *Biology of fibrous composites*. Cambridge, UK: Cambridge University Press.

Oliver, W. C. & Pharr, G. M. 1992 An improved technique for determining hardness and elastic modulus using load and displacement sensing indentation experiments. *J. Mater. Res.* **7**, 1564–1583.

Oliver, W. C. & Pharr, G. M. 2004 Measurement of hardness and elastic modulus by instrumented indentation: advances in understanding and refinements to methodology. *J. Mater. Res.* **19**, 3–20. (doi:10.1557/jmr.2004.19.1.3)

Paine, M. L., White, S. N., Luo, W., Fong, H., Sarikaya, M. & Snead, M. L. 2001 Regulated gene expression dictates enamel structure and tooth function. *Matrix Biol.* **20**, 272–292. (doi:10.1016/S0945-053X(01)00153-6)

Pharr, G. M. 1998 Measurement of mechanical properties by ultra-low load indentation. *Mater. Sci. Eng.* **A253**, 151–159.

Pontin, M. G., Moses, D. N., Waite, J. H. & Zok, F. W. Submitted. Continuous mechanical characterization of *Glycera* jaws utilizing nanoscratch and wear testing techniques.

Ratner, B. D., Hoffman, A. S., Schoen, F. J. & Lemons, J. E. 2004 *Biomaterials science*. London, UK: Elsevier.

Rho, J. Y., Tsui, T. Y. & Pharr, G. M. 1997 Elastic properties of human cortical and trabecular lamellar bone measured by nanoindentation. *Biomaterials* **18**, 1325–1330. (doi:10.1016/S0142-9612(97)00073-2)

Robinson, M. W., Colhoun, L. M., Fairweather, I., Brennan, G. P. & Waite, J. H. 2001 Development of the vitellaria of the liver fluke *Fasciola hepatica* in the rat host. *Parasitology* **123**, 509–518. (doi:10.1017/S0031182001008630)

Schaefer, J., Kramer, K. J., Garbow, J. R., Jacob, G. S., Stejskal, E. O., Hopkins, T. L. & Speirs, R. D. 1987 Aromatic cross-links in insect cuticle: detection by solid-state ^{13}C and ^{15}N NMR. *Science* **235**, 1200–1204.

Seto, J., Zhang, Y., Hamilton, P. & Wilt, F. 2004 The localization of occluded matrix proteins in calcareous spicules of sea urchin larvae. *J. Struct. Biol.* **148**, 1123–1130. (doi:10.1016/j.jsb.2004.04.001)

Stark, K. B., Gallas, J. M., Zajac, G. W., Golab, J. T., Gidanian, S., McIntire, T. & Farmer, P. J. 2005 Effect of stacking and redox state on optical absorption spectra of melanins-comparison of theoretical and experimental results. *J. Phys. Chem. B* **109**, 1970–1977. (doi:10.1021/jp046710z)

Szpoganicz, B., Gidanian, S., Kong, P. & Farmer, P. 2002 Metal binding by melanins: studies of colloidal dihydroxyindole–melanin, and its complexation by Cu(II) and Zn(II) ions. *J. Inorg. Biochem.* **89**, 45–53. (doi:10.1016/S0162-0134(01)00406-8)

Takeuchi, H. 2003 Raman structural markers of tryptophan and histidine side chain in proteins. *Biopolymers* **72**, 305–317. (doi:10.1002/bip.10440)

Taylor, S. W., Waite, J. H., Ross, M. M., Shabanowitz, J. & Hunt, D. F. 1994 *Trans*−2,3-*cis*-3,4-dihydroxyproline in the tandemly repeated consensus decapeptides of an adhesive protein from *Mytilus edulis*. *J. Am. Chem. Soc.* **116**, 10 803–10 804. (doi:10.1021/ja00102a063)

Vincent, J. F. V. 2002 Arthropod cuticle: a natural composite shell system. *Compos. Part A* **33**, 1311–1315. (doi:10.1016/S1359-835X(02)00167-7)

Vincent, J. F. V. & Wegst, U. 2004 Design and mechanical properties of insect cuticles. *Arthropod Struct. Dev.* **33**, 187–199. (doi:10.1016/j.asd.2004.05.006)

Vovelle, J. & Grasset, M. 1990 Données nouvelles sur la formation et la composition du tube larvaire de *Pectinaria* (= *Lagis*) *koreni* Malmgren (Annélide Polychète). *Cah. Biol. Mar.* **31**, 333–348.

Waite, J. H. 1990 The phylogeny and chemical diversity of quinone-tanned glues and varnishes. *Comp. Biochem. Physiol.* **B97**, 19–29.

Waite, J. H., Lichtenegger, H. C., Stucky, G. D. & Hansma, P. 2004 Exploring the molecular and mechanical gradients in structural bioscaffolds. *Biochemistry* **43**, 7653–7662. (doi:10.1021/bi049380h)

Wilson, K. & Walker, J. (eds) 2000 *Principles and techniques of practical biochemistry* 5th edn. Cambridge, UK: Cambridge University Press.

Williams, D. B. & Carter, C. B. 1996 *Transmission electron microscopy*. New York, NY: Plenum Press.

Wold, F. & Moldave, K. 1984 Posttranslational modifications. In *Part B in methods in enzymology* (ed. S. P. Colowick & N. O. Kaplan). Orlando, FL: Academic Press.

Wróblewski, K., Muhandiram, R., Chakrabartty, A. & Bennick, A. 2001 The molecular interaction of human salivary histatins with polyphenolic compounds. *Eur. J. Biochem.* **268**, 4384–4397. (doi:10.1046/j.1432-1327.2001.02350.x)

Zioupos, P., Tong Wang, X. & Currey, J. D. 1996 Experimental and theoretical quantification of the development of damage in fatigue tests of bone and antler. *J. Biomech.* **29**, 989–1002. (doi:10.1016/0021-9290(96)00001-2)